Egy. J. Pure & Appl. Sci. 2024; 62 (1):1-19

Egyptian Journal of Pure and Applied Science

Protective effect of *Punica granatum* peel extract and its alginate-encapsulated nanoparticles against acrylamide-induced neurotoxicity in rats

Asmaa M. Tawfek [1*], Asmaa S. EL-Houssiny [2], Omer A. Ahmed-Farid [3], Sahar B. Ahmed [4], Emad K. Ahmed [5], and Mahmoud M. Said [5]

[1] *Diagnostic Kits Department, Egyptian Drug Authority, Giza, Egypt.*

[2] *Microwave Physics and Dielectrics Department, National Research Centre, Giza, Egypt.*

[3] *Physiology Department, National Organization of Drug Control and Research (NODCAR), Giza, Egypt.*

[4] *Biochemistry Department, National Organization of Drug Control and Research (NODCAR), Giza, Egypt.*

[5] *Biochemistry Department, Faculty of Science, Ain Shams University, Cairo, Egypt.*

ARTICLE INFO

Received 7 November 2023
Accepted 5 December 2023

Keywords

Pomegranate peel extract ,
Alginate pomegranate peel extract nanoparticles,
Protective,
Acrylamide,
Brain injury.

Correspondence

Asmaa M. Tawfek

E-mail*

(Corresponding Author)

silentspring1292@gmail.com

ABSTRACT

The goal of the present study is to assess the possible protective effect of the pomegranate peel extract (PPE) and its alginate-nanoencapsulated form (Alg-PPE NPs) against rat neurotoxicity induced by acrylamide (ACR). The prepared Alg-PPE NPs were characterized using transmission electron microscopy (TEM), dynamic light scattering (DLS), zeta potential, Fourier transmission infrared microscopy (FITR), differential scanning calorimetry (DSC) as well as *in vitro* cytocompatibility and drug release analysis. The active ingredients of the two examined extracts were identified using HPLC analysis. ACR was intraperitoneally injected (50 mg/kg bw) three times per week for 2 consecutive weeks into male Wistar rats for the induction of neurotoxicity. PPE or Alg-PPE NPS were given in daily doses (200 mg/kg bw) orally for two consecutive weeks either individually or combined with acrylamide injection. Results revealed that ACR injection induced neurotoxicity manifested by the significant increase in tumor necrosis factor alpha, gamma aminobutyric acid, and DNA fragmentation level in brain tissues of treated animals. Meanwhile, the brain levels of brain-derived neurotrophic factor, total antioxidant capacity, acetylcholinesterase activity, dopamine, serotonin, norepinephrine, glutamine, glycine, and aspartate were significantly decreased. These changes in tissue biochemical parameters were associated with histopathological alternations in the architecture of brain tissues. Amelioration of the acrylamide-induced brain toxicity was observed following co-administration of either PPE or Alg-PPE NPs with a higher degree of protection observed with the nanoparticles form as a result of increased bioavailability. The protective effect of the studied extracts was ascribed mainly to the antioxidant potential of their phenolic and flavonoids components. In conclusion, Alg-PPE NPs can be regarded as a potential therapeutic agent that offers protection against acrylamide neurotoxicity, however, to fully understand the neuroprotective mechanism of Alg-PPE NPs at the molecular level, additional research must be done to characterize their active principles.

1. Introduction

When carbohydrate-rich foods, especially Western-style snacks, are cooked at high temperatures, acrylamide (ACR), a recognized water-soluble hazardous chemical, is produced. ACR has high permeability, making it simple to be absorbed during digestion via the digestive system and spread throughout the body by way of the circulatory system [1]. Accordingly, individuals are continuously exposed to minute levels of ACR found in meals throughout their lives, and its hazardous effects can be seen in a variety of tissues, including the brain [2]. In humans and laboratory animals, ACR causes peripheral and central neuropathy. A recent study has shown that ACR causes neuronal damage, alteration of neurotransmission, oxidative stress, and neuroinflammation that result in aberrant gait patterns and neurological impairments with the release of cytokines like interleukins (ILs) in response to oxidative stress [3]. Through the final decade, the use of pomegranate has increased due to its great taste and amazing health benefits. In the *Punicaceae* family, *Punica granatum* is known as the pomegranate.

The pomegranate fruit is known for its great antioxidant activity, antimicrobial, antiinflammatory, and anticancer properties due to its high concentration of bioactive phytochemicals. The peels represent approximately 50% of the *Punica granatum* fruit, and the antioxidant potential of pomegranate peel extract (PPE) is nearly 10 times greater than the other parts of the natural product [4]. The peels contain the highest concentration of polyphenolic compounds, basically hydrolysable ellagitannins, flavonoids, and anthocyanins. Ellagic acid, punicalin, punicalagin, and gallic acid are the dominant hydrolysable ellagitannins in the peels, and they are the constituents of the phytochemicals too, showing the most elevated antioxidant capacities [5, 6].

It has been reported that pomegranate peel is an amazing source of important biocompounds including hydrolysable tannins (gallic acids and ellagic acids, punicalagin, punicalin, and pedunculagin); phenolic acids (hydroxycinnamic acids and hydroxybenzoic); and flavonoids (anthocyanins, catechins, and other complex flavonoids) that show excellent beneficial effects on health [7]. Also, byproducts of pomegranate contain calcium, phosphorus, magnesium, potassium, and sodium, organic acids, protein, and mainly fatty acids as punicic, linoleic, and oleic acids present in the seeds [7].

Despite PPE's great health capacity, its use in functional foods is uncommon because tannin complexes with salivary glycoproteins, leading to sensory qualities that are totally disagreeable. In addition, PPE involvement with meals may reduce the functional benefits of substances used in the preparation or storage of food [8]. On the other hand, the pomegranate peel extract's application in different goods is complicated by its phenolic susceptibility to low pH, high temperatures, and light, as well as its metabolism in the gastrointestinal system. One of the essential tools in developing therapeutic systems is nanotechnology. Nanotechnology is used as a carrier for delivering compounds with therapeutic effects to increase the concentration of drugs in the target area [9].

The size range of nanoparticles (NPs) is both big enough to avoid renal and lymphatic-clearance and small enough to avoid opsonization. NPs are more likely to be taken up by cells than smaller or larger particles [10]. The natural polyphenolic compounds exhibit a low ability to cross the blood-brain barrier (BBB), which limits their therapeutic effects [11]. NPs has many advantages including high stability and extensive half-life in the blood-stream, shielding the contents against enzymatic degradation and hydrolysis, decreasing agitation of tissue due to the polymeric shell and improving bioavailability [4]. Alginate (a biodegradable and biocompatible co-polymer of guluronic acid and mannuronic acid extracted from brown seaweed) is frequently used for the encapsulation of various substances due to its availability, low cost, ease of gelation, and lack of toxicity.

Alginate has already received permission from the United States Food Drug Administration (US FDA) for human use and it is commonly administered orally. It is a non-immunogenic substance and has been used for wound healing, drug delivery, and tissue engineering applications. Furthermore, alginate hydrogel can effectively shield its contents from dangerous elements, and the calcium alginate beads were found to be effective when several plant extracts were encapsulated in them [12]. Therefore, the current study aimed to synthesize alginate-encapsulated nanoparticles of pomegranate (*Punica granatum*) peel extract (Alg-PPE NPs), as well as to assess its potential protective effect against acrylamide-induced brain injury in male rats.

2. Materials and Methods

2.1. Pomegranate peels

Pomegranate fruits (Punica granatum) were purchased from a local market (Cairo, Egypt). The fruits were peeled, and the peels were rinsed with distilled water, dried, ground using a grinder to powder and stored at 4° C until used.

2.2. Chemicals

Acrylamide (ACR) was obtained from Sigma Aldrich Company (Darmstadt, Germany). Sodium, alginate was purchased from ROTH (Karlsruhe, Germany). Calcium chloride, was purchased from Qualikems (New Delhi, India). All other chemicals were of pure analytical grades and purchased from Sigma Aldrich (Darmstadt, Germany) or Fluka companies (Milwaukee, USA).

2.3. Animals

Adult male outbred Wistar rats were obtained from the breeding animal house division of the National Organization for Drug Control and Research (NODCAR), Egyptian Drug Authority (EDA), Cairo, Egypt. Throughout the course of the experiment, the animals were kept in plastic cages under regular settings of temperature, humidity, and 12-hour light/dark cycles. They were fed a pelleted meal that included all the essential nutrients. Food and water were provided ad libitum throughout the study period and the rats were left to acclimatize for 1 week prior to the study. According to guidelines of Ethics Committee for Animal Experimentation at National Organization of Drug Control and Research (NODCAR) (Permit Num - BIO.92021), all procedures including animals handling were approved and performed.

2.4. Preparation of the ethanolic pomegranate peel extract (PPE)

Five hundred grams of the pomegranate peel powder were successively extracted three times with 80% ethanol. The pooled extracts were concentrated using a rotatory evaporator, filtered through Whatman filter paper (No. 2), and then freeze-dried. The yielded gummy residue was stored at -4°C for further analysis [13].

2.5. Preparations of alginate-pomegranate peel extract nanoparticles (Alg-PPE NPs)

Alginate-pomegranate peel extract nanoparticles (Alg-PPE NPs) were synthesized using a controlled gelification procedure depending on the polyanion's ionotropic gelation with CaCl2 [14]. Five hundred milligrams of sodium alginate were dissolved in one hundred milliliters distilled water at room temperature (5 mg/ml).

Five hundred milligrams extracted pomegranate peel were added to the alginate solution (concentration of 5 mg/ml), and mixed thoroughly for 24 hours. Following mechanical stirring, 5 ml of the solution containing calcium chloride (36 mM) were added to the alginate pomegranate peel extract mixture drop by drop while being constantly stirred to generate gelification. The suspension was further stirred for three hours at room temperature to obtain nanoparticles. The mean diameter of the Alg-PPE NPs was confirmed by transmission electron microscopy (TEM) and dynamic-light scattering (DLS). Eventually, the nanoparticles were freeze-dried for storage until use for characterization.

2.6. Preparation of acrylamide (ACR) solution

Acrylamide (ACR) was dissolved in saline (10% w/v). Each rat was interperitoneally injected with ACR (50 mg/kg bw) three times per week for two consecutive weeks [15].

2.7. Characterization of Alg-PPE NPs

2.7.1. Transmission electron microscope (TEM)

A transmission-electron microscope (TEM) with an acceleration voltage of 80 Kv (JEOL. JSM-100 CX, Japan) was used to measure the mean diameter of Alg-PPE NPs. A sample of the Alg-PPE NPs suspension was dropped onto a copper grid for TEM observations. The sample was stained with phosphotungstic acid after it had been completely dried [16].

2.7.2. Particle size analysis

The particle size of the Alg-PPE NPs was measured by dynamic-light scattering (DLS) using the Zeta sizer (Malvern instrument, UK). The mean value was calculated after measuring the particle size of a suspension of an aqueous solution of Alg-PPE NPs (1 mg/ml PPE) three times [17].

2.7.3. Zeta potential

A Zeta potential analyzer (Nicomp 380 ZLS, USA) was used to determine the Zeta potential value of the Alg NPs,, PEE, and Alg-PPE NPs. Prepared aqueous solutions of Alg NPs, Alg-PPE NPs, and PPE were tested at 1, 2, and 1 mg/ml, respectively. The average value was calculated after measuring each sample three times [18].

2.7.4. Attenuated total reflection-Fourier transform infrared spectroscopy (ATR-FTIR)

The ATR FTIR spectra of the Alg-NPs, Alg-PPE NPs and PPE were obtained using an ATR-FTIR (Bruker VERTEX 80, Germany) spectrophotometer associated with Platinum Diamond ATR- disc as an internal reflector. The samples were introduced onto the ATR crystal followed by acquisition of FTIR spectra over the scanning variety of 400-4000 cm−1 at a resolution of 4 cm-1 [19].

2.7.5. Differential scanning calorimetry (DSC)

The thermal behavior of Alg NPs, Alg-PPE NPs, and PPE was studied using differential scanning calorimetry (SETARAM Inc., France). To calibrate the instrument, various standards (Mercury, Indium, Tin, Lead, Zinc, and Aluminum) were utilized. The purging gases employed were nitrogen and helium. The test included a heating zone from room temperature to 300°C with a heating rate of 10°C/min. The samples were introduced to the DSC instrument after being weighed in aluminum pans. CALISTO Data program (v.149, Switzerland) was used to process the thermogram results [20].

2.8. In vitro cyto-compatibility of Alg-PPE NPs (MTT Assay)

Cell viability was determined by the mitochondrial dependent reduction of yellow 3-(4,5-dimethylthiazol-2-yl)-2,5-diphenyltetrazoliumbromide (MTT) to purple formazan crystals [21]. Normal retinal pigment epithelial cells (RPE1) were cultured in DMEM medium containing 1% antibiotic-antimycotic mixture (10,000 U/ml potassium penicillin, 10,000 µg/ml streptomycin sulfate, and 25 µg/ml amphotericin B) and 1% L-glutamine at 37 °C in 5 % CO2. After being batch cultured for 10 days, the cells were seeded at a density of 10×103 cells per well in fresh complete growth medium in 96-well microtiter plastic plates using a water jacketed carbon dioxide incubator (Sheldon, TC2323, Cornelius, OR, USA) at 37°C for 24 hour under 5% CO2. After adding fresh media devoid of serum, cells were either incubated alone (as a negative control) or in groups or with various concentrations of Alg-PPE NPs to achieve a final concentration of 100-50-25-12.5 µg/ml.

After 48 hours of incubation, the media were removed, and 40 µl of MTT salt (2.5 µg/ml) was added to each well. The experiment was then continued for a further 4 hours at 37°C and 5% CO2. To terminate the reaction and dissolve the crystals that had been formed, 200 µl of 10% sodium dodecyl sulphate (SDS) in deionized water were added to each well and incubated overnight at 37°C. A known cytotoxic natural agent (doxorubicin) with a concentration of 100 µg/ml was used as a positive control as it causes 100% lethality under the same circumstances [22]. The absorbance was then measured at 595 nm with a reference wavelength of 620 nm using a microplate multi-well reader (Bio-Rad Laboratories Inc., model 3350, Hercules, California, USA). The percentage of change in the cell viability was calculated according to the formula: [(Reading of sample/Reading of negative control) -1] × 100.

2.9. In vitro drug release study

Alg-PPE NPs were injected into the cellulose membrane of dialysis tubing (avg. flat width 25 mm, USA) in 250 ml beakers for the in vitro drug release study. The dialysis procedure was performed at room temperature with continuous magnetic stirring in 100 ml of phosphate buffer (pH 7.4). A volume of 2 ml aliquot was taken out and replaced with the same volume of brand-new buffer solution at predetermined regular intervals. A UV-Vis spectrophotometer (Jasco V-570, Japan) was used to spectrophotometrically analyze the samples that had been collected at the wavelength of maximum absorbance (360 nm). Plotting the cumulative amounts (Q) of pomegranate released from the Alg-PPE NPs as a function of time (hr) allowed researchers to determine the drug release profile [23].

2.10. Identification of polyphenolic compounds of PEE and Alg-PPE NPs by high performance liquid chromatography (HPLC)

The identification and estimation of polyphenolic compounds of PPE and Alg-PPE NPs by HPLC were carried out according to the method described by Abdel-Aziz et al. [24]. The mobile phase consists of solution A (HPLC grade water) and solution B (0.05 % trifluoracetic acid in acetonitrile). The HPLC conditions were UV detector at 280 nm (Agilent 1260 series, Santa Clara, USA), column (Eclipse C18 [4.6 mm×250 mm, 5µm]), flow rate (1 ml/min), injection volume (5 µl) and temperature (40°C).

2.11. Biological experiment and sample preparation

A total of 48 adult male Wistar rats were randomly divided equally into 6 groups and subjected to the following treatments. Control group in which animals were left intact and served as a normal control; ACR group in which rats were intraperitoneally (ip) injected with ACR (50 mg/kg bw) three times per week for 2 consecutive weeks [15]; PPE and Alg-PPE NPs groups in which rats were orally administered with PPE and Alg-PPE NPs (both dissolved in distilled water), respectively, in a daily dose equivalent to 200 mg/kg bw for two consecutive weeks [25]. The last two groups are protection groups comprising (PPE+ACR) and (Alg-PPE NPs+ACR) groups, in which rats were orally administered with PPE and Alg-PPE NPs (200 mg/kg bw), respectively, for two consecutive weeks and concomitantly ip injected with ACR (50 mg/kg bw) three times per week for 2 consecutive weeks.

At the end of the experiment, rats were killed by cervical dislocation, brains were excised at autopsy, rinsed in ice-cold saline, blotted dry with a filter paper and then dissected into 4 portions. The first part was used for the preparation of 10% w/v homogenate in 70% methanol to determine the levels of monoamine neurotransmitters (norepinephrine, dopamine and serotonin) and neurochemical amino acids (gamma amino butyric acid, aspartate, glutamine and glycine). The second part was preserved at -80ºC for DNA fragmentation assay, whereas the third part was homogenized in phosphate buffer (pH 7.4) for the analysis of tumor necrosis factor alpha (TNF-α), brain derived neurotropic factor (BDNF), total antioxidant capacity (TAC), as well as acetylcholinesterase (AChE) activity, whereas the last part was kept in 10 % formalin for histopathological analysis.

2.12. Biochemical analysis

Tumor necrosis factor-alpha (TNF-α) level was assessed in brain tissue homogenates using a rat specific kit (MyBioSource, California, United States) according to Dowlati et al. [26]. Brain derived neurotrophic factor (BDNF (level was assessed in brain tissue homogenates using a rat specific ELISA kit (Shanghai, China (according to Rostami et al. [27]. The total antioxidant capacity (TAC) (which considers the combined effect of all the antioxidants present) was measured in brain tissue homogenates according to the method of Koracevic et al. [28] using a kit provided by Biodiagnostics (Egypt). The activity of acetyl cholinesterase (AChE) in brain tissue homogenates was measured according to the method of Tietz et al. [29] using a colorimetric kit provided by Spinreact (Spain).

The measurement of brain monoamine neurotransmitters (norepinephrine, dopamine, and serotonin) using HPLC was done according to the method of Ogaly et al. [30]. Chromatographic conditions were as follows; Mobile phase: potassium phosphate (20 mM, pH 2.5), Column: AQUA column C18 (150 mm×4.6 mm, 5 µm from Phenomenex, USA), Flow rate: 1.5 ml/min, Detector: UV detector (Agilent 1260 series, Santa Clara, USA), Injection volume: 20 µl, Temperature: ambient. The brain tissue neurochemical amino acid contents (glutamine, glycine, gamma aminobutyric acid, and aspartate) were estimated by HPLC according to the method described by Heinrikson and Meredith [31].

Chromatographic conditions were as follows; Detector: UV detector (Agilent 1260 series, Santa Clara, USA), Column: PICO-TAG column C18 (30 cm×3.9 mm, 5 µm from Waters, Massachusetts, USA), Flow rate: 2 ml/min, Injection volume: 20 µl, Temperature: 46 °C. The report and chromatogram were taken from ChemStation program (Ohio, USA). The DNA content in the nucleic acids extract of brain tissue was determined by the diphenylamine method according to Perendones et al. [32].

2.13. Histopathological examination

Samples of brain tissues were fixed in formaldehyde solution (10 %) and then processed to form paraffin cubes. Paraffin wax tissue blocks were prepared for sectioning at 4 µm thickness by a sledge microtome. The obtained tissue sections were collected on glass slides, deparaffinized and stained by hematoxylin and eosin stain for histopathological examination through the electric light microscope [33].

2.14. Statistical analysis

All results were expressed as the mean ± standard deviation of the mean for eight animals in each group. CALISTO Data program (v.149, Switzerland) was used to process the thermogram results [20]. Subsequent multiple comparisons between different groups were employed using the post-hoc Duncan's test. The level of significancy was considered at p value of 0.05. The statistical analysis was done using Statistical Package for Social Science (SPSS) version 20.0 (SPSS Inc., Chicago, Il, USA).

3. Results and discussion

3.1. Characterization of alginate pomegranate peel extract nanoparticles (Alg-PPE NPs)

3.1.1. Particle size analysis

It is well known that the physicochemical characteristics of NPs, such as particle size and shape, are significant in cellular interactions and can influence both the non-specific uptake of NPs into cells and the behaviors of NPs in biological systems [34]. TEM analysis of the morphology and particle size of the prepared Alg-PPE NPs shows the presence of 8-12 nm sized tiny particles (Fig. 1-A). Additionally, the TEM view supported the existence of uniform, spherical nanoparticles with a smooth surface that did not aggregate.

TEM view also revealed that the Alg-PPE NPs are discrete, which may be related to the highly negative surface charge that is present and causes strong repellent interactions between the Alg NPs in dispersion, helping to prevent particle aggregation [35].
As shown in Fig. 1-B, the moderate particle size of Alg-PPE NPs measured by DLS is 27 nm, however, the NP size of Alg-PPE NPs measures 8-12 nm according to the TEM image. The NPs, therefore, seem smaller when observed by TEM as compared to DLS. Dehydration of the NPs during sample preparation for TEM imaging can be used to explain the difference between the two results. The apparent size (hydrodynamic radius) of a particle is measured by DLS, which also includes the hydrodynamic layers that surround Alg NPs. So, instead of measuring the actual diameter of hydrophilic NPs, the hydrodynamic diameter was measured by DLS.

3.1.2. Zeta potential

The cellular uptake of NPs is significantly influenced by the charge of the surface, which plays an important role in the cellular uptake, and can also affect how well the NPs adhere to cell membranes [36, 37]. Additionally, both *in vitro* and *in vivo*, it guides NPs to cellular compartments. A method called Zeta potential analyzes the total electric charge on the particle surface as well as the electrophoretic mobility of the individual particles. It also denotes the stability of the suspension, making it crucial for the NPs suspended in solution [38]. The PPE has a negative Zeta potential value of -14 mV (Fig. 2-A). Also, the Alg NPs moderate Zeta potential was -58.80 mV before PPE encapsulation (Fig. 2-B), and it changed to -83.63 mV after (Fig. 2-C).

The value of negative Zeta potential of Alg NPs may be attributed to the presence of ionized carboxyl groups on the Alg NPs surface. Typically, +30 mV or −30 mV is used as the common cutoff line between unstable and stable suspensions. Particles with Zeta potential greater than +30 mV or more negative than −30 mV are typically thought to be stable due to the surface charge [39]. The high surface charge of the prepared NPs is indicated by the high negative Zeta potential values observed for Alg NPs and Alg-PPE NPs. These surface charges lead to strong repellent interactions among the NPs in the dispersion. Therefore, high suspension stability is obtained for Alg NPs before and after encapsulation with PPE.

3.1.3. Attenuated total reflection-Fourier transformed infrared spectroscopy

The stability of the drug as well as any potential chemical interactions between it and nanoparticles can be investigated using FTIR spectroscopy. Any disappearance of the drug's FTIR peaks after being encapsulated indicates the drug-NPs interaction. The FTIR spectra of PPE, Alg-PPE NPs, and Alg NPs are shown in Fig. 2-D. Alg NPs' FTIR spectrum exhibits absorption bands at 3261 cm^{-1} attributed to O-H stretching, 2932 cm^{-1} attributed to C-H stretching, 1597 cm^{-1} and 1408 cm^{-1} corresponding to the asymmetric and symmetric stretching of carbonyl C=O, 1300 cm^{-1} attributed to C-C-H stretching, and 1129 cm^{-1} attributed to ether C-O-C stretching [40]. The FT-IR spectrum of pomegranate peel extract (PPE) demonstrates that the peel extract contains numerous compounds such as phenolic, carboxylic acids, alkenes, ethers, and others such as ellagic tannins gallic and ellagic acid esters. It shows absorption bands at 3277 cm^{-1} that corresponds to O-H stretching of polyphenols and flavonoids, and 2932 cm^{-1} due to the C-H stretching of alkenes.

The peaks at 1717 cm^{-1} and 1611 cm^{-1} correspond to carbonyl group C=O of carboxylic acids and N-H bending of amines. While the peaks at 1340, 1230 and 1027 cm^{-1} correspond to C-H stretching in alkanes or alkyl group, C-O groups stretching in ester, ether, or phenol group, and C-N stretching of aliphatic primary amine, respectively [41]. Meanwhile, in the spectrum of Alg-PPE NPs, the characteristic bands of Alg are not affected by the entrapment of PPE as they are slightly shifted from 1597 and 1408 cm^{-1} to 1600 and 1411 cm^{-1}, respectively. Hence, there is no new chemical bond formed between the functional group in the PPE and the Alg NPs. Therefore, PPE is physically entrapped in the Alg NPs without making any significant chemical interactions confirming the PPE stability and compatibility with Alg NPs during the encapsulation process. Moreover, in the spectrum of Alg-PPE NPs, there was a reduction in peak intensity at 1600 and 1411 cm^{-1} indicating the encapsulation of PPE within Alg NPs [42].

3.1.3. Differential Scanning Calorimetry (DSC)

To describe the physical state of the active components inside the nanoparticles, the DSC was used. DSC can reveal also the successful encapsulation of materials within the NPs. Generally, loss of any exo- or endothermic peaks indicates the perfect incorporation of the medication into the NPs.

The obtained PPE's DSC thermogram revealed a strong melting point at 50°C (Fig. 3-A) corresponding to volatilization of H_2O and the onset of melting of low-molecular weight compounds as phenolic substances and flavonoids. Meanwhile, the DSC thermogram of the Alg NPs (Fig. 3-B) revealed a sharp endothermic peak at 93°C, correlated with water loss from hydrophilic polymer groups that have not been completely removed during drying, then the degradation of the polymer due to dehydration and depolymerization events produced a pronounced exothermic peak at 244°C; this peak was most likely caused by partial decarboxylation of the protonated carboxylic groups and oxidation processes of the polymer. Conversely, the melting peak associated with PPE at 50°C was not visible on the DSC thermogram of the Alg-PPE NPs (Fig. 3-B), indicating that the PPE's crystalline structure had not yet formed and that the Alg-PPE NPs were in an amorphous condition. Furthermore, the Alg-PPE NPs did not exhibit the abrupt exothermic peak at 244 °C, but rather a depressed and broad peak as a result of mixing between the PPE and Alg NPs. Therefore, current results demonstrated the PPE's thermal compatibility and proved its effective encapsulation in the Alg NPs matrix [43].

3.2. In vitro cytocompatibility of the Alg-PPE NPs

Cell viability was assessed colorimetrically, quantitatively, and sensitively using the MTT assay [21]. A typical retinal pigment epithelial cell line (RPE1) was used to test the *in vitro* cytotoxicity of the Alg-PPE NPs (Fig. 4-A). The cell viability of the cells treated with various concentrations of the analyzed NPs samples was slightly influenced, and was only dropped by 16% for the maximum concentration of the generated NPs. Commonly, it is well accepted that a substance is considered cytotoxic when it results in a 30% or more reduction in cell viability [44]. Alginate is actually a widely used polymer with low cytotoxicity, strong biocompatibility, and biodegradability since the byproducts of its biodegradation are harmless and non-toxic [45]. These outcomes validated the Alg-PPE NPs' cytocompatibility.

3.3. In vitro drug release studies

The *in vitro* drug release profile of pomegranate peel extract from Alg NPs up to 24 hour is shown in Fig. 4-B. It is noted that the *in vitro* release of PPE from Alg NPs is a biphasic linear profile with an initial fast release of about 54 % during the first 7 hr, followed by a more gradual and sustained release phase up to 91 % over 24 h.

This suggests that the developed Alg-PPE NPs can be used as an important platform for sustained drug release applications. The initial fast release is a result of free PPE adsorbed on the surface of Alg NPs and the rapid hydration of Alg NPs. whereas the sustained release is attributed to those PPE molecules crosslinked with the nanoparticle network by $CaCl_2$. Also, at higher pH 7.4 of the PBS, a greater amount of carboxylic acid salt (–COO−) was produced, thus leading to increased electrostatic repulsion of inter- and intramolecules, and therefore increasing the pore size and cumulative release of Alg-PPE NPs [46].

3.4. Identification of the active ingredients in PPE and Alg-PPE NPs by HPLC analysis

HPLC analysis was used for the identification and quantitative analysis of some various phenolic compounds in pomegranate peel extract and Alg-PPE NPs (Tables 1 & 2). In the ethanol extract of pomegranate peels and Alg-PPE NPs, compounds of nine polyphenolic, including syringic acid, chlorogenic acid, catechin, ellagic acid, methyl gallate, caffeic acid, gallic acid, ferulic acid, and naringenin, were identified. Gallic acid was the most abundant (30688.98 µg/g) followed by catechin (7601.35 µg/g), ellagic acid (6779.57 µg/g) and chlorogenic (5664.84 µg/g), while ferulic acid (170.46 µg/g), syringic acid (123.17 µg/g), methyl gallate (107 µg/g), caffeic acid (98.37 µg/g), and naringenin (248.47 µg/g) were the lowest abundant in the ethanol extract of pomegranate peels.

For Alg-PPE NPs, catechin (3733.24 µg/g) was the most abundant followed by ellagic acid (3137.29 µg/g), chlorogenic (2796.02 µg/g) and gallic acid (2267.81 µg/g), while caffeic acid (186 µg/g), methyl gallate (63.64 µg/g), syringic acid (60.85 µg/g), ferulic acid (13.96 µg/g), and naringenin (173.48 µg/g) were the lowest abundant. Previous reports have shown that the antioxidant capabilities of pomegranate peel extracts were mostly ascribed on the presence of considerable levels of phenolic and flavonoid components (such as ellagic and gallic acids) [47]. Present findings agree with several other studies that detected high levels of total polyphenols, flavonoids, and anthocyanins in the methanol extracts of various components of *Punica granatum* [48-50]. The present findings also firmly establish that phenolics are significant elements of the pomegranate peel, and at least part of their pharmacological actions could be ascribed to the presence of these key elements.

3.5. The protective effect of PPE and Alg-PPE NPs against ACR induced neurotoxicity

Rats orally administered with either PPE or Alg-PPE NPs extracts did not show significant changes in any of the tested biochemical parameters (Tables 3-5), except for a slight reduction in brain's AChE activity, compared to untreated rats. Also, the sole administration of either PPE or Alg-PPE NPs exerted no significant changes on the percent of DNA fragmentation in brain tissues. Further, brain sections revealed non-significant histopathological alterations in the neuron structure after two weeks of either PPE or Alg-PPE NPs administration (Fig. 5). These findings support the safety of the examined extracts. Similar observations have been reported previously for pomegranate peel extracts [51, 52]. Intoxication of male rats with acrylamide produced a sharp significant increase in the level of brain TNF-α, GABA, and % DNA fragmentation compared to untreated controls. Meanwhile, the levels of BDNF, TAC, AChE activity, DA, NE, 5-HT, Gln, Gly, and Asp decreased significantly in the brain of ACR-treated rats, compared to their respective controls (Tables 3-5). These changes in tissue biochemical parameters were associated with histopathological alterations in the architecture of brain tissue (Fig. 5).

These elevations and reductions of the tested parameters have been previously described and were attributed to the ACR-induced neurotoxicity and neuron damage [15]. According to reports, biochemical indices and micromorphological alterations in tissues exposed to ACR demonstrate that ACR induces production of free radicals with subsequent oxidative stress accompanied by changes in tissue architecture [53, 54]. The brain tissue is much more at risk for ROS-induced lipid peroxidation than other tissues because of having a greater content of polyunsaturated fatty acids, a lower rate of antioxidant defense, a reduced ability for regeneration, and a relatively high oxygen consumption rate [55]. ACR monomer has been shown to be neurotoxic, genotoxic, carcinogenic, and to cause developmental and reproductive damage in laboratory animals [56]. ACR interacts with reduced glutathione to create conjugates in biological systems, and the resulting complex is then broken down by cytochrome P450 (subtype CYP 2E1) to produce glycidamide (GA), which is harmful to essential macromolecules like proteins and DNA. High dosages of acrylamide alter enzyme activity and the state of oxidation, greatly escalating oxidative stress [58].

The expression of COX-2 and nitric oxide synthase in breast epithelial cells was similarly observed to be increased by ACR [59]. Increased COX-2 expression is known to cause a series of inflammatory reactions that may lead to apoptosis and ultimately cell death [15]. Ataxia, skeletal muscle weakness, and weight loss are the hallmarks of ACR-induced neuropathy in both experimental animals and humans [60]. The participation of oxidative stress processes and inflammatory responses has been hypothesized [61] despite the fact that the fundamental mechanisms of ACR-induced neuropathy are not fully understood. In the current study, in addition to the significant decrease in the total antioxidant capacity and the sharp increase in the proinflammatory cytokine TNF-α, acrylamide intoxication significantly reduced brain-derived neurotrophic factor (BDNF) suggesting that loss or alterations in it may contribute to neuronal dysfunction in ACR neurotoxicity. BDNF is a vital member of the neurotrophins family that acts on specific neurons in the peripheral and central nervous systems to support the survival of pre-existing neurons and promote the growth and differentiation of new neurons and synapses [62].

The current results also revealed a significant reduction in AChE activity in brain tissue due to ACR treatment. Similar findings have been previously observed and were attributed to the production of free radicals and adducting presynaptic protein thiol groups by ACR with subsequent disruption of the antioxidant balance within the brain [63, 64]. Also, the concentration of GABA in brain tissues was increased due to current ACR neurotoxicity. It has been reported that GABA increases can cause damage to tardive neurons by enhancing inhibitory synapses. Additionally, GABA increases can cause damage to neurons by enhancing inhibitory synapses [65]. According to these findings, ACR may decrease glutamate concentrations by increasing GAD65 expression [2]. ACR also caused a considerable decrease in the levels of brain serotonin and dopamine. A variety of factors have been proposed to explain such reduction including ACR interaction with tyrosine and tryptophan, the precursor amino acids for DA and 5-HT synthesis, together with raising the level of monoamine oxidase enzyme in the rat brain which is crucial for the breakdown of monoamine neurotransmitters [66]. This may provide evidence that the reduced brain monoamine levels seen in rats treated with ACR may be due to active degradation.

In comparison to controls, current exposure to ACR significantly enhanced the level of DNA fragmentation in brain cells. The potential of ACR to produce reactive oxygen species could be considered the principal cause of this impact [67]. The ACR-generated ROS are extremely active free radicals that damage biological macromolecules like DNA. The oxidative damage caused by free radical-mediated DNA damage is the initial step in mutagenesis, carcinogenesis, and ageing. ACR treatment also caused alterations in the architecture of brain tissue such as the extensive shrunken hypereosinophilic damaged neurons in the prefrontal cortex and the edema in the neuropil (Fig. **5**). Amelioration of the acrylamide-induced toxicity was observed following coadministration of either PPE or Alg-PPE NPs with acrylamide treatment, as demonstrated by the significant ameliorative reduction in the brain's TNF-α, GABA, and % DNA fragmentation together with significant ameliorative elevation of the brain BDNF, TAC, AChE activity, NE, 5-HT, Gln, Gly, and Asp levels, compared to acrylamide-treated rats.

In all the determinations, a higher degree of protection against acrylamide intoxication was recorded following Alg-PPE NPs treatment (Tables **3-5**). Several studies have shown that the proinflammatory cytokines, such as TNF-α, IFN-β, and IL-6 are increased by free radical-mediated apoptotic mechanisms [68]. It was hypothesized that antioxidants and free radical scavengers could counteract this effect, which supports our findings indicating that cotreatment with pomegranate peel extracts and acrylamide overcame the effects of acrylamide concerning the release of cytokines and inflammatory mediators. The present lowering effect of the levels of the proinflammatory cytokine TNF-α due to pomegranate peel extracts was also reported by Toklu et al. [69].

In fact, separate studies demonstrated pomegranate peel extracts to have both antioxidant and antimutagenic properties [70]. Polyphenols have been shown to be responsible for the antioxidant activity of plant extracts [71]. The prepared pomegranate peel extracts are rich in a variety of phenolic substances (Tables **1** & **2**). Ellagic acid is one of the main active identified components which has previously demonstrated prominent biological activities in different studies, such as anti-oxidation, antitumor, anti-inflammatory, neuroprotection, anti-viral, and anti-bacterial [8].

Also, pomegranate ellagitannins, punicalagin and ellagic acid were reported to have potent antioxidant, anti-atherosclerotic and anticancer activities [72]. The free radical scavenging activity of pomegranate peel phenols involves electron donation to free radical that converts them to relatively more stable compounds. The antioxidant power of pomegranate peel extract has been found to linearly increase with the concentration of peel phenolics [70]. In fact, great therapeutic options have been related to plant-derived phytochemicals due to their therapeutic potential in several human disorders [73]. Reports highlighted the biological potentials of these phytochemicals, through different antioxidant and anti-inflammatory activities, in counteracting neurodegeneration [74].

Phenolic compounds are prominent promising sources for the treatment and resistance of age-related neurodegeneration. The development of new therapeutic applications to increase their bioavailability and efficacy is a major concern of several research groups [75]. Previous reports have demonstrated the outstanding neuroprotective potentials of several phenolic compounds [76-78]. In addition, phenolic compounds have been demonstrated to exhibit exceptional bioactivity in a variety of ageing- and neurodegenerative-related pathogenic processes, including downregulation of oxidative stress and proinflammatory cytokine expression, regulation of apoptosis, and activation of proteolysis pathways like the UPS to prevent protein aggregation [79].

Further, flavonoids have been shown to minimize apoptosis, amyloidogenic effects, and loss of dopaminergic neurons, as well as to limit ROS generation, improve the expression of antioxidant proteins, neuron survival, and cerebral blood flow [80]. Also, phenolic acids have been shown to improve a variety of conditions, including epilepsy, neuroinflammation, apoptosis, memory problems, excitotoxicity, and depression [81]. The administration of phenolic compounds highlights a potential alternative for the treatment of neurodegenerative pathologies [79]. Brain delivery using alginate-formulated nanoparticles have been previously reported. Alginate-cholesterol micelles coated with lactoferrin were shown to be able to deliver a neuroprotective steroid to the brain [82]. Also, venlafaxine-loaded alginate nanoparticles (VLF AG-NPs) were shown to improve brain delivery of an anti-depressant [83].

We therefore suggest that alginate nano-encapsulation of PPE improved the delivery of polyphenol compounds across the BBB and enhance their intracellular uptake into the target cells, which warrants further investigation. Therefore, the current ameliorative potential of PPE against ACR-induced brain toxicity could be attributed to its high content of polyphenol compounds and flavonoids. Interestingly, a higher degree of protection was achieved through the encapsulation of PPE. This suggests that the encapsulation of PPE with alginate as a carrier helps to improve the bioavailability and biological activity of PPE polyphenols.

The improvement of polyphenol bio-accessibility may potentially increase their absorption, resulting in achieving systematic concentration and demonstrating higher antioxidant and anti-inflammatory activities leading to a higher degree of protection. In fact, nano-encapsulation of polyphenol compounds was reported to increase the antioxidant and the anti-inflammatory power compared to the non-encapsulated forms [84]. The neuroprotective and antioxidant properties of the two examined extracts were clearly observed in reducing the histopathological changes caused by ACR in the brain tissues manifested by the greater number of intact neurons in most layers of the parietal cortex with few degenerated cells (Fig. 5).

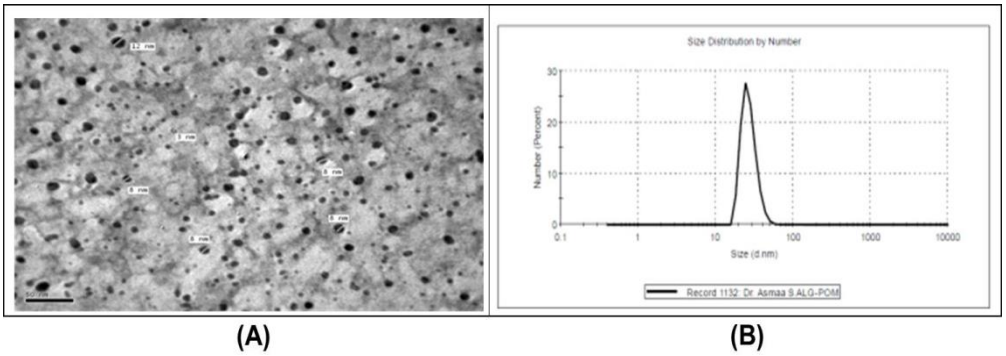

Fig. 1 (A) A TEM image of Alg-PPE NPs solution and its particle size distribution (27 nm) (B).

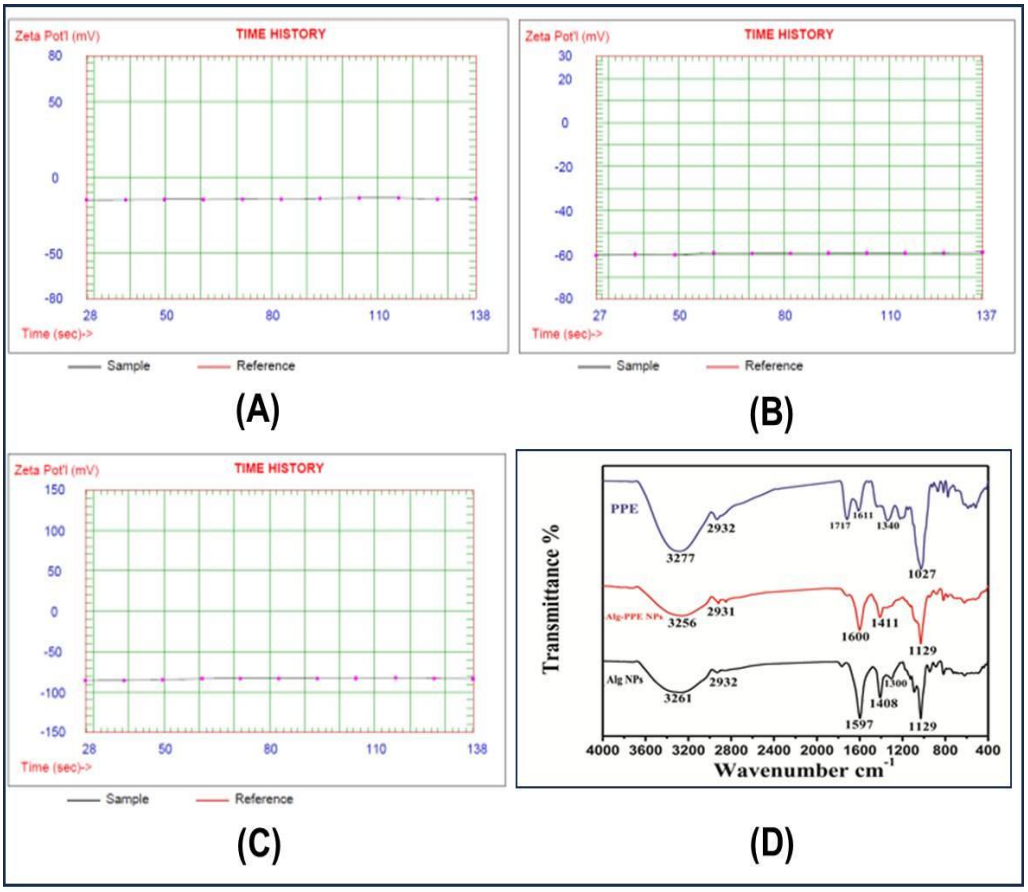

Fig. 2 (A) Zeta potential of PPE (-14 mV), (B) Zeta potential of Alg NPs (-58.80 mV), (C) Zeta potential of Alg-PPE NPs (-83.63 mV), (D) FT-IR spectra of Alg NPs, Alg-PPE NPs and PPE.

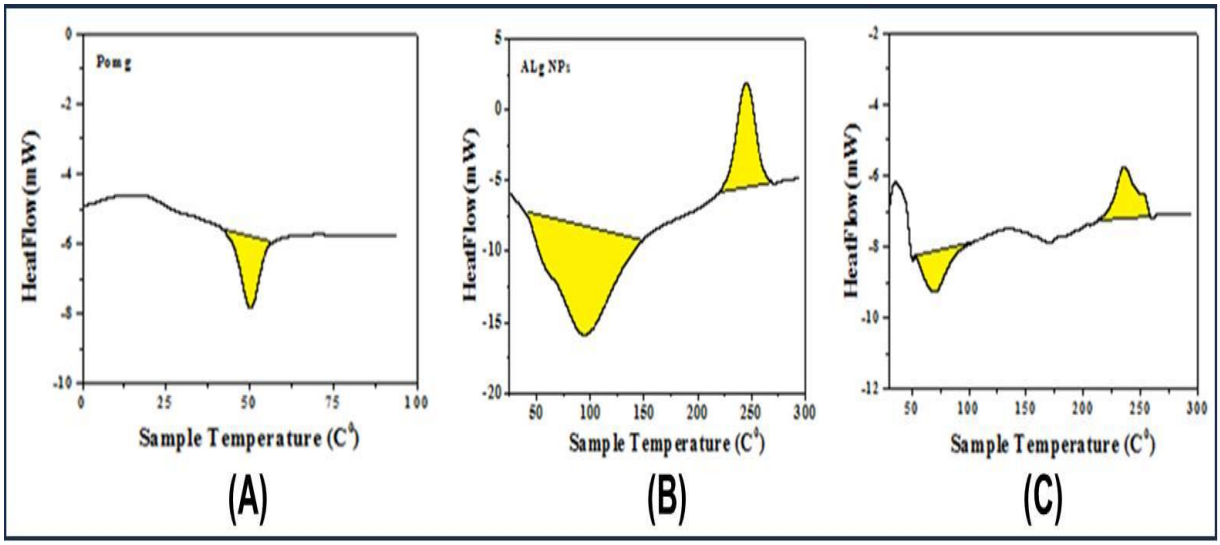

Fig. 3 DSC thermogram of PPE (A), Alg NPs (B), and Alg-PPE NPS (C).

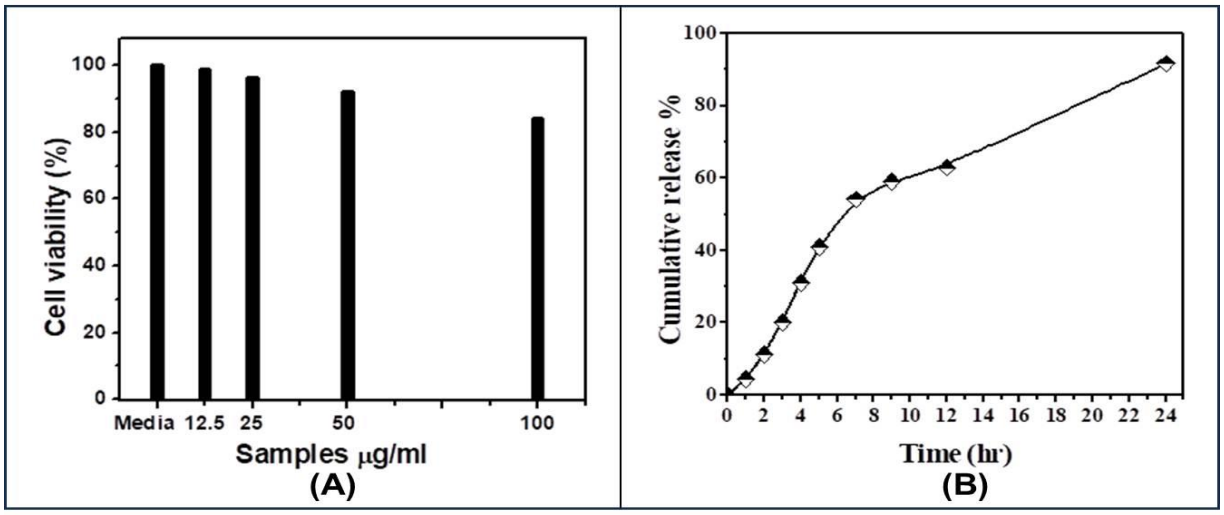

Fig. 4 *In vitro* cytocompatibility of Alg-PPE NPs (A) and *in vitro* drug release of PPE (B).

Table 1. The concentration of phenolic compounds identified in the ethanol extract of PPE by HPLC

Compound	Retention time (min)	Area	Area %	Conc. (µg/g)
Gallic acid	3.710	2613.43	60.430	30688.98
Chlorogenic	3.956	573.74	13.260	5664.84
Catechin	4.165	547.01	12.640	7601.35
Methyl gallate	4.928	66.00	1.525	107.89
Caffeic acid	5.437	21.03	0.486	98.37
Syringic acid	5.958	22.40	0.518	123.17
Pyro catechol	6.082	ND	0	ND
Rutin	7.299	ND	0	ND
Ellagic acid	8.022	387.84	8.967	6779.57
Coumaric acid	8.253	ND	0	ND
Vanillin	8.920	19.90	0.460	54.36
Ferulic acid	9.571	35.37	0.817	170.46
Naringenin	10.020	38.42	0.888	248.47
Quercetin	12.190	ND	0	ND
Cinnamic acid	13.300	ND	0	ND
Kaempferol	14.230	ND	0	ND
Hesperetin	14.740	ND	0	ND
Total		100%		

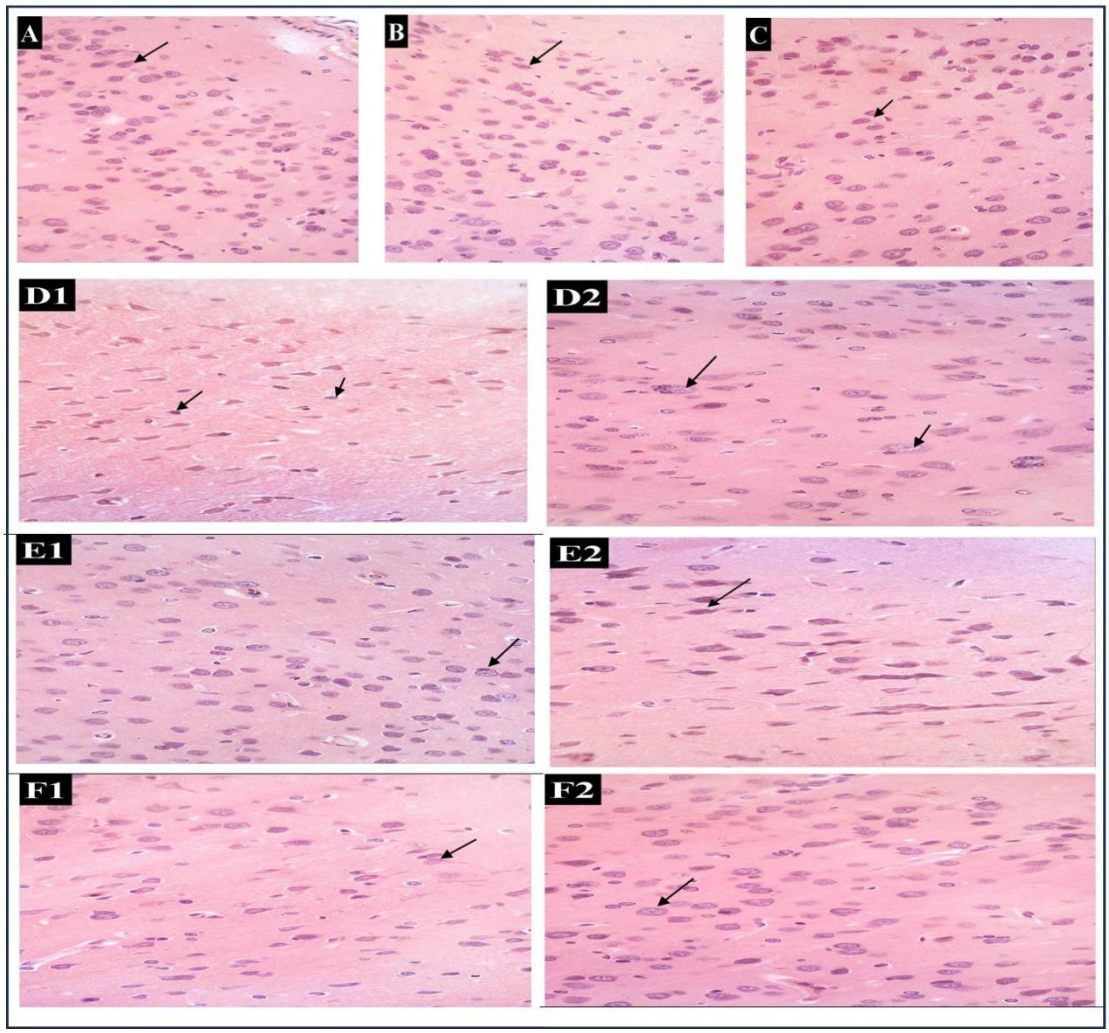

Fig. 5 Photomicrographs of rat brain sections Photomicrographs of rat brain sections from the control group (A), the PPE group (B), and the Alg-PPE NPs group (C) stained with hematoxylin and eosin show normal histological structures of different cortical regions and layers with apparent intact neurons and normal cellular details (arrows). Intact intercellular tissues with a few scattered glial cells are seen. D1 and D2 are photomicrographs of rat brain sections from the ACR group showing extensive shrunken hypereosinophilic damaged neurons in the prefrontal cortex, accompanied by mild edema in the neuropil. Focal areas of damaged pyknotic neurons were shown in the outer layers of the parietal cortex (arrows). However, most of the deeper cortical layers are apparently intact. E1 and E2 are photomicrographs of rat brain sections from the PPE+ACR group showing many apparent intact neurons in most layers of the parietal cortex with few degenerated cells. Focal areas of damaged pyknotic neurons are shown in the outer layers of the parietal cortex (arrows). F1 and F2 are photomicrographs of rat brain sections from the Alg-PPE NPs+ACR group showing many apparent intact neurons in most of the layers of the parietal cortex with few degenerated cells. However, the prefrontal cortex showed alternate areas of intact and degenerated neurons in the outer cortical zone, with more protected deeper cortical zones (arrows) (×400).

Table 2. The concentration of phenolic compounds identified in the Alg-PPE NPs by HPLC

Compound	Retention time (min)	Area	Area %	Conc.(µg/g)
Gallic acid	3.620	2191.29	69.074	2267.81
Chlorogenic	3.952	321.40	10.131	2796.02
Catechin	4.168	304.91	9.611	3733.24
Methyl gallate	5.011	44.19	1.392	63.64
Caffeic acid	5.359	45.13	1.422	186.00
Syringic acid	5.965	12.56	0.396	60.85
Pyro catechol	6.082	ND	0	ND
Rutin	7.299	ND	0	ND
Ellagic acid	8.031	203.70	6.421	3137.29
Coumaric acid	8.253	ND	0	ND
Vanillin	8.918	10.86	0.342	26.12
Ferulic acid	9.562	3.29	0.103	13.96
Naringenin	10.100	30.45	0.959	173.48
Quercetin	12.190	ND	0	ND
Cinnamic acid	13.430	4.59	0.144	ND
Kaempferol	14.230	ND	0	ND
Hesperetin	14.740	ND	0	ND
Total		100%		

Table 3. The change in the brain levels of TNF-α, BDNF, TAC and AChE activity among different groups

Groups	TNF-α (pg/g tissue)	BDNF (pg/g tissue)	TAC (mM/g tissue)	AChE (U/g tissue)
Control	50.62 ± 1.55^{A}	36.31 ± 2.19^{A}	0.85 ± 0.03^{A}	216.70 ± 9.6^{A}
ACR	109.75 ± 0.6^{B}	18.77 ± 0.81^{B}	0.40 ± 0.06^{B}	128.73 ± 7.7^{B}
PPE	50.34 ± 2.11^{A}	35.84 ± 1.92^{A}	0.81 ± 0.04^{A}	191.45 ± 12.3^{CD}
Alg-PPE NPs	49.88 ± 2.42^{A}	37.23 ± 2.18^{A}	0.81 ± 0.04^{A}	198.47 ± 12.6^{D}
PPE + ACR	74.94 ± 3.34^{C}	28.59 ± 2.62^{C}	0.52 ± 0.02^{C}	175.94 ± 7.7^{E}
Alg-PPE NPs + ACR	56.94 ± 2.85^{D}	32.94 ± 1.62^{D}	0.67 ± 0.06^{D}	187.19 ± 10.7^{CF}

Data are represented as Mean ± SD of eight observations. Values with dissimilar superscripts are considered significantly different. ANOVA test followed by Duncan's multiple comparisons among different groups at $p < 0.05$ was applied.

Table 4. The change in the brain NE, DA, 5HT, Glu, Gly, GABA and ASP levels among different groups

Groups	NE (µg/g tissue)	DA (µg/g tissue)	5-HT (µg/g tissue)	Glu (µg/g tissue)	Gly (µg/g tissue)	GABA (µg/g tissue)	ASP (µg/g tissue)
Control	0.52 ± 0.02^{A}	0.72 ± 0.04^{A}	0.53 ± 0.05^{A}	4.23 ± 0.38^{A}	9.79 ± 0.33^{A}	5.93 ± 0.44^{A}	2.05 ± 0.15^{A}
ACR	0.21 ± 0.01^{B}	0.46 ± 0.01^{B}	0.22 ± 0.03^{B}	2.3 ± 0.23^{B}	4.73 ± 0.17^{B}	10.87 ± 0.587^{B}	1.21 ± 0.12^{B}
PPE	0.50 ± 0.05^{A}	0.70 ± 0.02^{A}	0.51 ± 0.06^{A}	4.01 ± 0.28^{A}	9.56 ± 0.82^{A}	5.20 ± 0.37^{A}	1.95 ± 0.09^{A}
Alg-PPE NPs	0.49 ± 0.06^{A}	0.69 ± 0.04^{A}	0.53 ± 0.03^{A}	4.01 ± 0.27^{A}	9.06 ± 1.22^{A}	5.14 ± 0.24^{A}	1.97 ± 0.13^{A}
PPE+ACR	0.31 ± 0.02^{C}	0.53 ± 0.02^{C}	0.32 ± 0.03^{C}	2.87 ± 0.25^{C}	6.45 ± 0.78^{C}	8.13 ± 0.40^{C}	1.61 ± 0.32^{C}
Alg-PPE NPs + ACR	0.45 ± 0.02^{D}	0.64 ± 0.03^{D}	0.46 ± 0.03^{D}	3.29 ± 0.26^{D}	7.23 ± 1.00^{C}	7.20 ± 0.38^{D}	1.76 ± 0.16^{C}

Data are represented as Mean ± SD of eight observations. Values with dissimilar superscripts are considered significantly different. ANOVA test followed by Duncan's multiple comparisons among different groups at $p < 0.05$ was applied.

Table 5. The change in the brain DNA percentage (%) fragmentation among different groups

Groups	% DNA
Control	20.01 ± 0.54^{A}
ACR	40.75 ± 0.85^{B}
PPE	21.83 ± 0.25^{A}
Alg-PPE NPs	23.25 ± 0.85^{A}
PPE + ACR	27.50 ± 1.76^{C}
Alg-PPE NPs + ACR	26.25 ± 1.72^{C}

Data are represented as Mean ± SD of eight observations. Values with dissimilar superscripts are considered Significantly different. ANOVA test followed by Duncan's multiple comparisons among different groups at $p < 0.05$ was applied.

4. Conclusion

A model of acrylamide-induced bran toxicity in rats was verified in the current study, and possible neuroprotective effects of pomegranate peel extract (PPE) and its alginate-encapsulated nanoparticles (Alg-PPE NPs) were recorded. The encapsulation process was conducted, and the developed nanoparticles were analyzed in terms of structure, cytocompatibility, and drug release. Both extracts succeeded in attenuating acrylamide-induced neurotoxicity and the neuroprotective effect was more pronounced for Alg-PPE NPs because of increased bioavailability of its polyphenol and flavonoids components. Alg-PPE NPs supplementation can be regarded as a potential strategy that offers protection against acrylamide neurotoxicity, especially for people who work in industries that make or use acrylamide and have higher exposures through skin contact or inhalation. However, further study is needed to establish the bioavailability and biological activity of Alg-PPE NPs under physiological conditions in the human body.

5. Conflicts of interest

The authors declare there are no conflicts of interest.

6. References

1. **Bicer, Y., Elbe, H., Karayakali, M., Yigitturk, G., Yilmaz, U., Cengil, O., Al Gburi, M. R. A. and Altinoz, E. (2022).** Neuroprotection by melatonin against acrylamide-induced brain damage in pinealectomized rats. J Chem Neuroanat., **125: 102143.**
2. **Tian, S. M., Ma, Y. X., Shi, J., Lou, T. Y., Liu, S. S. and Li, G. Y. (2015).** Acrylamide neurotoxicity on the cerebrum of weaning rats. Neural Regen Res., **10 (6): 938-43.**
3. **Pang, Y., Chen, J., Yang, J., Xue, Y., Gao, H. and Gao, Q. (2023).** Protective effect and mechanism of Lycium ruthenicum polyphenols against acrylamide-induced neurotoxicity. Food Funct., **14(10): 4552-4568.**
4. **Andishmand, H., Azadmard-damirchi, S., Hamishekar, H., Torbati, M. A., Kharazmi, M. S., Savage, G. P., Tan, C. and Jafari, S. M. (2023).** Nano-delivery systems for encapsulation of phenolic compounds from pomegranate peel. Adv Colloid Interface Sc., **311: 102833.**
5. **Salim, A., Deiana, P., Fancello, F., Molinu, M. G., Santona, M. and Zara, S. (2023).** Antimicrobial and antibiofilm activities of pomegranate peel phenolic compounds: Varietal screening through a multivariate approach. Journal of Bioresources and Bioproducts., **8 (2): 146-161.**
6. **Gigliobianco, M. R., Cortese, M., Nannini, S., Nicolantonio, L. D., Peregrina, D. V., Lupidi, G., Vitali, L. A., Bocchietto, E., Martino, P. D. and Censi, R. (2022).** Chemical, Antioxidant, and Antimicrobial Properties of the Peel and Male Flower By-Products of Four Varieties of Punica granatum L. Cultivated in the Marche Region for Their Use in Cosmetic Products. Antioxidants (Basel)., **11(4): 768.**
7. **Pirzadeh, M., Caporaso, N., Rauf, A, Shariati, M. A, Yessimbekov, Z., Khan, M. U., Imran, M. and Mubarak, M. S. (2021).** Pomegranate as a source of bioactive constituents: a review on their characterization, properties and applications. Crit Rev Food Sci Nutr., **61 (6): 982-999.**

8. **Xiang, Q., Li, M., Wen, J., Ren, F., Yang, Z., Jiang, X. and Chen, Y. (2022).** The bioactivity and applications of pomegranate peel extract: A review. J Food Biochem., **46 (7): e14105.**
9. **Wang, L., Jiang, Y. S. J., Zhang, C. L. H., Zhang, X., Jiang, T., Wang, L., Wang, Y. and Feng, L. (2022).** Micro-Nanocarriers Based Drug Delivery Technology for Blood-Brain Barrier Crossing and Brain Tumor Targeting Therapy. Small., **18 (45): e2203678.**
10. **Anselmo, A. C. and Mitragotri, S. (2019).** Nanoparticles in the clinic: An update. Bioeng Transl Med., **4(3): e10143.**
11. **Ramalho, M. J., Andrade, S., Loureiro, J. A. and Pereira, M. D. C.(2020).** Nanotechnology to improve the Alzheimer's disease therapy with natural compounds. Drug Deliv Transl Res., **10 (2): 380-402.**
12. **Wongverawattanakul, C., Suklaew, P. O., Chusak, C., Adisakwattana, S. and Thilavech, T. (2022).** Encapsulation of Mesona chinensis Benth Extract in Alginate Beads Enhances the Stability and Antioxidant Activity of Polyphenols under Simulated Gastrointestinal Digestion. Foods., **11 (15): 2378.**
13. **Ahmed, M. M. and Ali, E. S. (2010).** Protective effect of pomegranate peel ethanol extract against ferric nitrilotriacetate induced renal oxidative damage in rats. Journal of Cell and Molecular Biology., **7(2): 35-43.**
14. **Rajaonarivony, M., Vauthier, C., Couarraze, G., Puisieux, F. and Couvreur, P. (1993).** Development of a new drug carrier made from alginate. J Pharm Sci., **82 (9): 912-7.**
15. **Prasad, S. N., and Muralidhara. (2013).** Neuroprotective efficacy of eugenol and isoeugenol in acrylamide-induced neuropathy in rats: behavioral and biochemical evidence. Neurochem Res., **38 (2): 330-45.**
16. **Monnier, C. A., Thévenaz, D. C., Balog, S., Fiore, G. L., Vanhecke, D., Rothen-Rutishauser, B. and Petri-Fink, A. A. (2015).** guide to investigating colloidal nanoparticles by cryogenic transmission electron microscopy: pitfalls and benefits. AIMS Biophysics., **2 (3): 245-258.**
17. **Goudarzi, H. R., Mokarram1, A. R., Noofeli1, M. , Shirvan1, A. N. and Saadati. (2016).** Preparation and evaluation of alginate nanoparticles containing pertussis toxin as a particulate delivery system. Biology, Materials Science., **7 (2): 558-564.**
18. **El-Houssiny, A. S., Fouad, E. and Hegazi, A. (2021).** A Comparative Antimicrobial Activity Study of Moringa oleifera Extracts Encapsulated within ALg Nanoparticles. Nanoscience and Nanotechnology – Asia., **11(1): 144-152.**
19. **El-Houssiny, A., Kamel, N.A., Soliman, A. A. F., Abd El-Messieh1, S. L. and Abd-EL-Nour, K. N. (2022).** Preparation and characterisation of gallic acid loaded carboxymethyl chitosan nanoparticles as drug delivery system for cancer treatment. Adv. Nat. Sci: Nanosci. Nanotechnol **13 (2): 025002.**
20. **Farag, T. K., El-Houssiny, A. S., Abdel-Rahman, E. H. and Hegazi, A. G. (2020).** A new approach to the treatment of lumpy skin disease infection in cattle by using propolis encapsulated within alg nps. Advances in Animal and Veterinary Sciences., **8(12): 1346-1355.**
21. **Mosmann, T. (1983).** Rapid colorimetric assay for cellular growth and survival: application to proliferation and cytotoxicity assays. J Immunol Methods., **65 (1-2): 55-63.**
22. **Thabrew, M. I., Hughes, R. D. and McFarlane, I. G. (1997).** Screening of hepatoprotective plant components using a HepG2 cell cytotoxicity assay. J Pharm Pharmacol., **49 (11): 1132-5.**
23. **El-Houssiny, A. S., Ward, A. A. , Mostafa, D. M., Abd-El-Messieh, S. L., Abdel-Nour, K. N., Darwish, M. M. and Khalil, W. A. (2017).** Sodium alginate nanoparticles as a new transdermal vehicle of glucosamine sulfate for treatment of osteoarthritis. European Journal of Nanomedicine., **9 (3-4): 105-114.**
24. **Abdel-Aziz, A-W. A., Elwan, N. M., Abdallah, M. A., Shaaban, R. S., Osman, N. S. and Mohamed, M. A-M.(2021).** High-Performance Liquid Chromatography-Fingerprint Analyses, In vitro Cytotoxicity, Antimicrobial and Antioxidant Activities of the Extracts of Ceiba speciosa Growing in Egypt. Egyptian journal of chemistry., **64 (4): 1831-1843.**

25. **Abdel Moneim, A. E. (2012).** Evaluating the potential role of pomegranate peel in aluminum-induced oxidative stress and histopathological alterations in brain of female rats. Biol Trace Elem Res., **150 (1-3): 328-36.**
26. **Dowlati, Y., Herrmann, N., Swardfager, W., Liu, H., Sham, L., Reim, E. K. and Lanctôt, K. L. (2010).** A meta-analysis of cytokines in major depression. Biol Psychiatry., **67(5): 446-57.**
27. **Rostami, S., Haghparast, A. and Fayazmilani, R. (2021).** The role of pre-pubertal training history on hippocampal neurotrophic factors and glucocorticoid receptor protein levels in adult male rats. Neurosci Lett., **752: 135834.**
28. **Koracevic, D., Koracevic, G., Djordjevic, V., Andrejevic, S. and Cosic, V. (2001).** Method for the measurement of antioxidant activity in human fluids. J Clin Patho., **54(5): 356-61.**
29. **Tietz, N. W. (1995).** Clinical guide to laboratory tests, in Clinical guide to laboratory tests. **1096-1096.**
30. **Ogaly, H. A., Ogaly, Abdel-Rahman, R. F., Mohamed, M. A-E, Ahmed-Farid, O. A., Khattab, M. S. and Abd-Elsalam, R. M. (2022).** Thymol ameliorated neurotoxicity and cognitive deterioration in a thioacetamide-induced hepatic encephalopathy rat model; involvement of the BDNF/CREB signaling pathway. Food Funct., **13 (11): 6180-6194.**
31. **Heinrikson, R. L. and Meredith, S. C. (1984).** Amino acid analysis by reverse-phase high-performance liquid chromatography: precolumn derivatization with phenylisothiocyanate. Anal Biochem., **136(1): 65-74.**
32. **Perandones, C. E., Illera, V. A., Peckham, D. and Stunz, L. L. (1993).** Ashman, R. F. Regulation of apoptosis in vitro in mature murine spleen T cells. J Immunol., **151(7): 3521-9.**
33. **Banchroft, J., Stevens, A. and Turner, D. .J. .N. Y. (1996).** Theory and practice of histological techniques Fourth Ed Churchil Livingstone.
34. **Chithrani, B. D., Ghazani, A. A. and Chan, W. C. (2006).** Determining the size and shape dependence of gold nanoparticle uptake into mammalian cells. Nano Lett., **6 (4): 662-668.**
35. **Moradhaseli1, S., Mirakabadi, A. Z., Sarzaeem, A., Dounighi, N. M., Soheily, S. and Borumand, M. R. (2013).** Preparation and characterization of sodium alginate nanoparticles containing ICD-85 (venom derived peptides). International journal of innovation and applied studies., **4(3): 534-542.**
36. **Chen, C. C., Tsai, T-H., Huang, Z-R. and Fang, J-U. (2010).** Effects of lipophilic emulsifiers on the oral administration of lovastatin from nanostructured lipid carriers: physicochemical characterization and pharmacokinetics. Eur J Pharm Biopharm., **74 (3): 474-482.**
37. **Patil, S., Sandberg, A., Heckert, E., Self, W. and Seal, S. (2007).** Protein adsorption and cellular uptake of cerium oxide nanoparticles as a function of zeta potential. Biomaterials., **28 (31): 4600-4607.**
38. **Yang, S-G., Chang, J-E., Park, S. Na. and Shim C-K. (2010).** 99mTc-hematoporphyrin linked albumin nanoparticles for lung cancer targeted photodynamic therapy and imaging. Journal of material chemistry., **20 (41): 9042-9046.**
39. **Zielińska, A., da Ana, R., Fonseca, J., Szalata, M., Wielgus, K., Fathi, F., Oliveira, M. B. P. P., Staszewski, R., Karczewski, J. and Souto, E. P. (2023).** Phytocannabinoids: Chromatographic Screening of Cannabinoids and Loading into Lipid Nanoparticles. Molecules., **28 (6): 2875.**
40. **Daemi, H. and Barikani, M.J.S.I. (2012).** Synthesis and characterization of calcium alginate nanoparticles, sodium homopolymannuronate salt and its calcium nanoparticles. Molecules., **19 (6): 2023-2028.**
41. **Goudarzi, M., Mir, N., Mousavi-Kamazani, M., Bagheri, S. and Salavati-Niasari, M. (2016).** Biosynthesis and characterization of silver nanoparticles prepared from two novel natural precursors by facile thermal decomposition methods. Sci Rep., **6: 32539.**
42. **Sohail, R. and Abbas, S. R. (2020).** Evaluation of amygdalin-loaded alginate-chitosan nanoparticles as biocompatible drug delivery carriers for anticancerous efficacy. Int J Biol Macromol., **153: 36-45.**

43. **El-Houssiny, A., Ward, A. A., Mostafa, D. M., Abd-El-Messieh, S. L., Abdel-Nour, K. N., Darwish, M. M. and Khalil, W. A. (2016).** Drug–polymer interaction between glucosamine sulfate and alginate nanoparticles: FTIR, DSC and dielectric spectroscopy studies. Advances in Natural Sciences: Nanoscience and Nanotechnology., **7(2): 025014.**
44. **Thangaraju, P. and Varthya, S. B. (2022).** biological evaluation of medical devices, in Medical device guidelines and regulations handbook. Springer., **163-187.**
45. **Cheaburu-Yilmaz, C. N., Lupuşoru, C. E. and Vasile, C. (2019).** New Alginate/PNIPAAm Matrices for Drug Delivery. Polymers (Basel)., **11(2), 366.**
46. **Chun, W., Xiong, F. and LianSheng, Y. (2007).** Water-soluble chitosan nanoparticles as a novel carrier system for protein delivery. Springer., **52: 883-889.**
47. **El-Hadary, A .E. and Taha, M. (2020).** Pomegranate peel methanolic-extract improves the shelf-life of edible-oils under accelerated oxidation conditions. Food science and nutrition., **8(4): 1798-1811.**
48. **Sadeghipour, A., Eidi, M., Kavgani, A. I., Ghahramani, R. and Shahabzadeh, S., (2014).** Anissian, A. Lipid Lowering Effect of Punica granatum L. Peel in High Lipid Diet Fed Male Rats. Evid Based Complement Alternat Med., **2014: 432650.**
49. **Middha, S. K., Usha, T. and Pande, V. (2013).** A Review on Antihyperglycemic and Antihepatoprotective Activity of Eco-Friendly Punica granatum Peel Waste. Evid Based Complement Alternat Med., **2013: 656172.**
50. **Elfalleh, W., Hannachi, H., Tlili, N., Yahia, Y., Nasri, N. and Ferchichi, A. (2012).** Total phenolic contents and antioxidant activities of pomegranate peel, seed, leaf and flower. Journal of Medicinal Plants Research., **6 (32): 4724-4730.**
51. **Hosseini, B., Saedisomeolia, A., Wood, L. G., Yaseri, M. and Tavasoli, S. (2016).** Effects of pomegranate extract supplementation on inflammation in overweight and obese individuals: A randomized controlled clinical trial. Complementary therapies in clinical practice., **22: 44-50.**
52. **Mena, P., García-Viguera, C., Navarro-Ric, J., Moreno, D. A., Bartual, J., Saura, D. and Martí N. (2011).** Phytochemical characterisation for industrial use of pomegranate (Punica granatum L.) cultivars grown in Spain. J Sci Food Agric., **91(10): 1893-906.**
53. **Batoryna, M., Lis, M. and Formicki, G.(2017).** Acrylamide-induced disturbance of the redox balance in the chick embryonic brain. J Environ Sci Health., **B 52(8): 600-606.**
54. **Farouk, S. M., Gad, F. A., Almeer, R., Abdel-Daim, M. M. and Emam, M. A. (2021).** Exploring the possible neuroprotective and antioxidant potency of lycopene against acrylamide-induced neurotoxicity in rats' brain. Biomed Pharmacother., **138: 111458.**
55. **Celik, H., Kucukler, S., Ozdemir, S., Comakli, S., Gur, C., Kandemir, F. M. and Yardim, A. (2020).** Lycopene protects against central and peripheral neuropathy by inhibiting oxaliplatin-induced ATF-6 pathway, apoptosis, inflammation and oxidative stress in brains and sciatic tissues of rats. Neurotoxicology., **80: 29-40.**
56. **Tardiff, R. G., Gargas, M. L., Kirman, C. R., Carson, M. L. and Sweeney, L. M. (2010).** Estimation of safe dietary intake levels of acrylamide for humans. Food Chem Toxicol., **48 (2): 658-667.**
57. **Dybing, E., Farmer, P. B., Andersen, M., Fennel, T. R., Lalljie, S. P. D., Müller, D. J. G., Olin, S., Petersen, B. J., Schlatter, J., Scholz, G., Scimeca, J. A., Slimani, N., Törnqvist, M., Tuijtelaars, S. and Verger, P. (2005).** Human exposure and internal dose assessments of acrylamide in food. Food Chem Toxicol., **43(3): 365-410.**
58. **Teodor, V., Cuciureanu, M., Filip, C., Zamosteanu, N. and Cuciureanu, R. (2011).** Protective effects of selenium on acrylamide toxicity in the liver of the rat. Effects on the oxidative stress. Rev Med Chir Soc Med Nat Iasi., **115(2): 612-8.**
59. **Lyn-Cook, L. E., Tareke, E.,Word, B., Starlard-Davenport, A., Lyn-Cook, B. D. and Hammons, G. J. (2011).** Food contaminant acrylamide increases expression of Cox-2 and nitric oxide synthase in breast epithelial cells. Toxicol Ind Health., **27(1):11-8.**

60. **Lehning, E. J., Balaban, C. D., Ross, J. F., Reid, M. A. and LoPachin, R. M. (2002).** Acrylamide neuropathy. I. Spatiotemporal characteristics of nerve cell damage in rat cerebellum. Neurotoxicology., **23(3): 397-414.**
61. **Lim, T. G., Lee, B. K., Kwon, J. Y., Jung, S. and Lee, K. W. (2011).** Acrylamide up-regulates cyclooxygenase-2 expression through the MEK/ERK signaling pathway in mouse epidermal cells. Food Chem Toxicol., **49(6): 1249-54.**
62. **Girotra, P., Behl, T., Sehgal, A., Singh, S. and Bungau, S. (2022).** Investigation of the Molecular Role of Brain- Derived Neurotrophic Factor in Alzheimer's Disease. Journal of Molecular Neuroscience Neurosci., **72(2): 173-186.**
63. **Zhang, T., Zhang, C., Luo, Y., Liu, S., Li, S., Li, L., Ma, Y. and Liu, J. (2023).** Protective effect of rutin on spinal motor neuron in rats exposed to acrylamide and the underlying mechanism. Neurotoxicology., **95: 127-135.**
64. **Haridevamuthu, B., Manjunathan, T., Guru, A., Alphonse, C. R. W., Boopathi, S., Murugan, R., Gatasheh, M. K., Hatamleh, A. A., Juliet ,A., Gopinath, P. and Arockiaraj, J. (2022).** Amelioration of acrylamide induced neurotoxicity by benzo[b]thiophene analogs via glutathione redox dynamics in zebrafish larvae. Brain Res., **1788: 147941.**
65. **Aboubakr, M., Ibrahim, S. S., Said, A. M., Elgendey, F. and Anis, A. (2019).** Neuroprotective effects of clove oil in acrylamide induced neurotoxicity in rats. Pakistan Veterinary Journal., **39(1): 111-115.**
66. **Rawi, S. M., Mohamed-Assem. Marie S., Fahmy, S. R. and El-Abied, S. A. (2012).** Hazardous effects of acrylamide on immature male and female rats. African Journal of Pharmacy and Pharmacology., **6(18): 1367-86.**
67. **Mehri, S., Abnous, K., Mousavi, S. H., Shariaty, V. M. and Hosseinzadeh, H. (2012).** Neuroprotective effect of crocin on acrylamide-induced cytotoxicity in PC12 cells. Cell Mol Neurobiol., **32 (2): 227-35.**
68. **Sayed, S., Alotaibi, S. S., El-Shehawi, A. M., Hassan, M. M., Shukry, M., Alkafafy, M. and Soliman, M. (2022).** The Anti-Inflammatory, Anti-Apoptotic, and Antioxidant Effects of a Pomegranate-Peel Extract against Acrylamide-Induced Hepatotoxicity in Rats. Life (Basel)., **12(2): 224.**
69. **Toklu, H. Z., Sehirli, O., Ozyurt, H., Mayadağli, A. A., Ekşioğlu-Demiralp, E., Cetinel, S., Sahin, H., Yeğen, B. C., Dumlu, M. U., Gökmen, V. and Sener, G. (2009).** Punica granatum peel extract protects against ionizing radiation-induced enteritis and leukocyte apoptosis in rats. J Radiat Res., **50(4): 345-53.**
70. **Negi, P., Jayaprakasha, G. and Jena, B. J. F. C. (2003).** Antioxidant and antimutagenic activities of pomegranate peel extracts. Food chemistry., **80(3): 393-397.**
71. **Orozco-Villafuerte, J., Alvarez-Ramirez, J., Buendía-González, L., García-Morales, C., Hernandez-Jaimes, C. and Alvarez-Ramirez, J. (2018).** Evaluation of the protection and release rate of bougainvillea (Bougainvillea spectabilis) extracts encapsulated in alginate beads. Journal of dispersion science and technology., **40(7): 1065-1074.**
72. **Seeram, N. P., Adams, L. S., Henning, S. M., Niu, Y., Zhang, Y., Nair, M. G. and Heber, D. (2005).** In vitro antiproliferative, apoptotic and antioxidant activities of punicalagin, ellagic acid and a total pomegranate tannin extract are enhanced in combination with other polyphenols as found in pomegranate juice. J Nutr Biochem., **16(6): 360-7.**
73. **Fierascu, R. C., Sieniawska, E., Ortan, A., Fierascu, I. and Xiao, J. (2020).** Fruits By-Products - A Source of Valuable Active Principles. A Short Review. Front Bioeng Biotechnol., **8: 319.**
74. **Limanaqi, F., Biagioni, F., Mastroiacovo, F., Polzella, M., Lazzeri, G. and Fornai, F. (2020).** Merging the Multi-Target Effects of Phytochemicals in Neurodegeneration: From Oxidative Stress to Protein Aggregation and Inflammation. Antioxidants (Basel)., **9 (10):1022.**
75. **Figueira, I., Garcia, G., Pimpão, R. C., Terrasso, A. P., Costa, I., Almeida, A. F., Tavares, L., Pais, T. F., Pinto, P., Ventura, M. R., Filipe, A., McDougall, G. J., Stewart, D., Kim, K. S., Palmela, I., Brites, D., Brito, M. A., Brito, C. and Santos, C. N.(2017).** Polyphenols journey through blood-brain barrier towards neuronal protection. Sci Rep., 7 (1): 11456.

76. **Maurya, H. (2019).** Research Article Neuroprotective Potential of Swietenia macrophylla Seed Extract in Lead-induced Neurodegeneration in Albino Rats. Asian Journal of Biological Sciences., **12: 442-449.**
77. **Dos Santos, L. C., Mendiola, J. A., Sanches-Camargo, A. D. P., Álvarez-Rivera, G., Viganó, J., Cifuentes, A., Ibáñez, E. and Martínez, J. (2021).** Selective Extraction of Piceatannol from Passiflora edulis by-Products: Application of HSPs Strategy and Inhibition of Neurodegenerative Enzymes. Int J Mol Sci., **22 (12): 6248.**
78. **Roy, S. and Bhat R. (2019).** Suppression, disaggregation, and modulation of γ-Synuclein fibrillation pathway by green tea polyphenol EGCG. Protein Sci., **28 (2): 382-402.**
79. **Rojas-García, A., Fernández-Ochoa, A., Cádiz-Gurrea, M. D. E. L., Arráez-Román, D. and Segura-Carretero, A. (2023).** Neuroprotective Effects of Agri-Food By-Products Rich in Phenolic Compounds. Nutrients., **15 (2): 449.**
80. **Meng-Zhen, S., Ju, L., Lan-Chun, Z., Cai-Feng, D., Shu-da, Y., Hao-Fei, Y. and Wei-Yan, H. (2022).** Potential therapeutic use of plant flavonoids in AD and PD. Heliyon., **8 (11): e11440.**
81. **Szwajgier, D., Borowiec, K. and Pustelniak, K. (2017).** The Neuroprotective Effects of Phenolic Acids: Molecular Mechanism of Action. Nutrients., **9 (5), 477.**
82. **Zheng S, Xie Y, Li Y, Li L, Tian N, Zhu W, Yan G, Wu C, Hu H. (2014).** Development of high drug-loading nanomicelles targeting steroids to the brain. Int J Nanomedicine, **9:55-66.**
83. **Haque, S., Md, S., Sahni, J.K., Ali, J. and Baboota, S., (2014).** Development and evaluation of brain targeted intranasal alginate nanoparticles for treatment of depression. J Psychiat Res., **48(1): 1-12.**
84. **Trindade, L. R., da Silva, D.V. T., Baião, D. D. S. and Paschoalin, V. M. F. (2021).** Increasing the Power of Polyphenols through Nanoencapsulation for Adjuvant Therapy against Cardiovascular Diseases. Molecules., **26 (15): 4621.**